Available online at www.sciencedirect.com

SciVerse ScienceDirect

Ceramics International 39 (2013) 5949–5954

CERAMICS INTERNATIONAL

www.elsevier.com/locate/ceramint

Short communication

Thermally grown TiO_2 nanowires to improve cell growth and proliferation on titanium based materials

B. Dinan[a], D. Gallego-Perez[b,c,d], H. Lee[a], D. Hansford[b,c,d], S.A. Akbar[a,*]

[a]*Department of Materials Science and Engineering, The Ohio State University, Columbus, OH 43210, USA*
[b]*Department of Biomedical Engineering, The Ohio State University, Columbus, OH 43210, USA*
[c]*NSF Nanoscale Science and Engineering Center, The Ohio State University, Columbus, OH 43210, USA*
[d]*Ohio Nanotech West Laboratory, The Ohio State University, Columbus, OH 43210, USA*

Received 31 October 2012; received in revised form 2 December 2012; accepted 3 December 2012
Available online 7 January 2013

Abstract

Titanium dioxide (TiO_2) nanowires (NWs) grown by thermal oxidation were investigated as a means of improving cell adhesion and proliferation of human osteosarcoma (HOS) cells on Ti 6 wt% Al–4 wt% V (Ti64) substrates. The TiO_2 NWs were grown on thermally spray coated Ti64 by a simple oxidation process. HOS cell proliferation was observed on bare Ti64 and both nanostructured and non-nanostructured TiO_2 surfaces by fluorescence microscopy and laser scanning cytometry (LSC). The alkaline phosphatase (ALP) activity of the HOS cells was also monitored at regular intervals. The NW coated samples showed increased cell adhesion and proliferation compared to the non-nanostructured TiO_2 and Ti64 samples. This investigation has demonstrated the feasibility of using a simple oxidation process to produce NWs as a means of coating Ti64 based devices to increase cell adhesion and proliferation.

Keywords: B. Whiskers; D. TiO_2; E. Biomedical applications; E. Functional applications

1. Introduction

Titanium dioxide (TiO_2) one dimensional (1-D) nanostructures have been the focus of much research due to the enhanced electronic and optical properties, quantum confinement effects, and increased surface area they can provide [1,2]. These 1-D TiO_2 nanostructures have been utilized in a variety of applications, including chemical sensing, photocatalysis, and photovoltaics [3–6]. Previously we have reported a one-step growth process to produce TiO_2 nanowires (NWs) on titanium alloys by thermal oxidation [7]. In this manuscript we present the results of the application of this growth process as a means of improving cell adhesion/proliferation on Ti64 (6 wt % Al–4 wt % V) based biomedical implants.

Ti and Ti64 have been widely used for biomedical applications such as hip joint replacements and dental implants due to their mechanical and chemical stabilities and their biocompatibility [8]. However, the bioactivity of bare Ti and Ti64 surfaces has been shown to be relatively low, which results in reduced cell/tissue–implant interactions, and subsequently leads to implant failure [8]. Surface modifications of the Ti based implants have been shown to enhance cell–implant interactions by increasing the surface area [9,10]. There have been reports of direct depositions of coatings such as TiO_2 and hydroxyapatite (HA) on Ti or Ti64 plates to improve the bioactivity [9]. However, HA coatings are reported to have poor adhesion to the metal as well as poor mechanical stability in the body [11]. As an alternative, TiO_2 coatings deposited by thermal spray methods have been employed to increase the surface area of the implants [12]. In the present study, Ti64 samples thermally spray coated and oxidized to produce a coating of 1-D NWs were seeded with human osteosarcoma (HOS) cells. Cell behavior was compared to that on uncoated

*Correspondence to: Department of Materials Science and Engineering, The Ohio State University, 2041 North College Road, 295B Watts Hall, Columbus, OH, 43210, USA. Tel.: +1 614 292 6725; fax: +1 614 688 4949.
E-mail address: akbar.1@osu.edu (S.A. Akbar).

0272-8842/$ - see front matter © 2012 Elsevier Ltd and Techna Group S.r.l. All rights reserved.
http://dx.doi.org/10.1016/j.ceramint.2012.12.004

Ti64 metal and spray coated TiO_2 film coated samples. The HOS cells showed increased cell adhesion and proliferation on the TiO_2 NW coated Ti64 samples.

2. Materials and methods

2.1. Ti64 substrates

Ti64 (grade 5, Ti–6 wt% Al–4 wt% V; OnlineMetals, Seattle, WA) metal bars were cut to approximately 2 cm × 2 cm × 1 cm coupons using a diamond cutter (LECO, part number 801-136) and mechanically polished using SiC sand paper (1200 grit). After polishing, all samples were cleaned by the following procedure including a rinse in deionized (DI) water between each step: (1) 5 min ultrasonication in acetone, (2) 5 min untrasonication in methanol, and (3) 5 min ultrasonication in DI water.

2.2. TiO_2 coating on Ti64 samples by thermal spray

TiO_2 coated Ti64 samples were obtained from Dr. Lima at National Research Council of Canada and the coating process is described as follows. TiO_2 coatings were fabricated by a high velocity oxy-fuel (HVOF) technique on a Ti64 substrate. The powder for the TiO_2 coatings had a particle size distribution from 5 to 20 μm and was obtained from Altair Nanomaterials Inc. The metal substrates were grit-blasted to roughen the surface before spraying for the purpose of increasing adhesion between the TiO_2 coating and the Ti64 substrate. The powder was thermally sprayed for 2 min on the metal substrates via an HVOF technique using an oxy-propylene based torch. The coatings were approximately 100 μm and black-gray in appearance. The coating's crystal phase was identified as a mixture of rutile and anatase by X-ray diffraction (XRD) with the dominant phase being rutile. More detailed information about the coatings and coated film characterization can be found elsewhere [12].

2.3. Oxidation

The oxidation process used to create the TiO_2 NW samples is similar to the methods previously reported [7]. Briefly, TiO_2 coated Ti64 samples were inserted into a quartz tube (OSU Glass Shop) which was then placed in a horizontal tube furnace (Lindberg, TF55035A) for gas heat treatments. Laboratory grade (4.8) argon gas was introduced into the reaction chamber at a flow rate of 500 mL/min using a digital flow meter (C100L, Sierra Instruments). The furnace was then ramped to the target temperature and maintained for a specified duration before air quenching to room temperature by opening the furnace. To promote NW growth, the oxidation temperature was set to 700 °C and held for 8 h under the previously described gas environment.

2.4. Specimen characterization

A field emission scanning electron microscope (FEG-SEM, Model Sirion, FEI, Oregon) was used for high resolution observation to detect changes in the surface morphology of the specimens at sub-micron scales. Prior to SEM characterization, samples were coated with a thin layer of Au using a sputter coater (Model 3 Sputter Coater

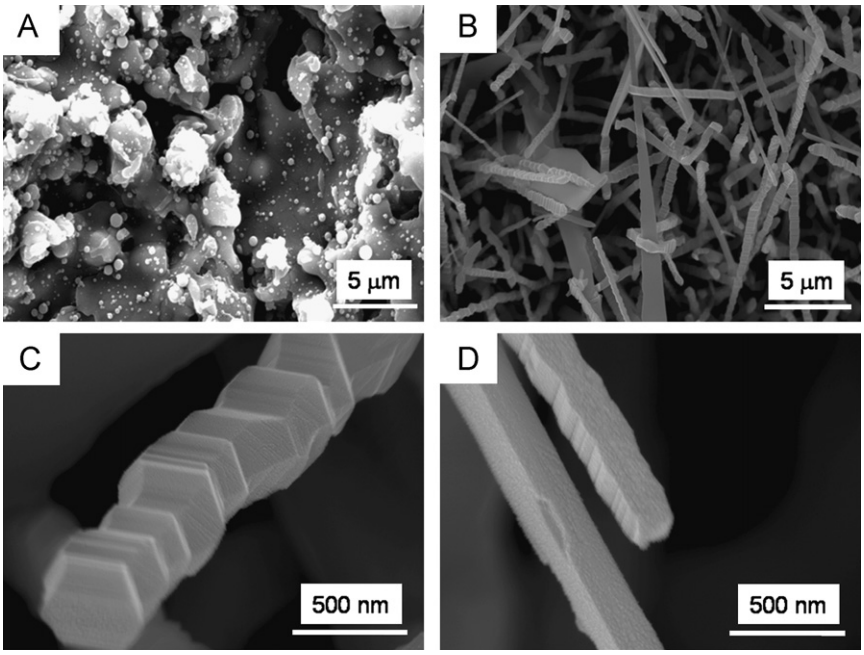

Fig. 1. (A) Surface image of TiO_2 coating on Ti64 before, and (B) after oxidation at 700 °C for 8 h. (C) A SEM micrograph showing a NW consisting of polyhedrons, and (D) an image showing a nanoribbon with smooth top surface and rippled sides.

91000, PELCO) at a plasma current of ~15 mA for 40 s. Crystal structure verification was performed using XRD analysis (Scintag PAD-V and Bruker XD) prior to Au coating. The structure of the resulting NWs was examined with a high resolution transmission electron microscope HRTEM (Model 4000EX, JEOL) at an operation voltage of 400 kV. Elemental analysis of individual NWs was performed by electron dispersive spectroscopy (EDS) in a high resolution TEM (HRTEM, Model TF20) operating in the scanning mode. The NWs were collected on a lacy carbon coated copper TEM grid by scraping the specimen with a razor blade and dispersing in ethanol. Droplets of the nanowire containing solution were placed on a carbon-coated copper grid and dried at 40 °C in a drying oven (Lindburg, M01430A).

2.5. Cytocompatibility testing

Surface cytocompatibility was evaluated by seeding human osteosarcoma (HOS) cells (ATCC, USA) on the previously sterilized (by autoclaving) specimens at a density of 5×10^4 cells/cm^2. Flat substrates of polished Ti64 (Ti64), Ti64 coated on a thermally grown TiO_2 film (designated as TiO_2) and Ti64 thermally oxidized to produce TiO_2 NWs (designated as TiO_2 NWs) were used for comparison. The cells were cultured for 15 h as well as 10, 25, and 35 days (medium changed every 2 days).

Alkaline phosphatase (ALP) activity, an early marker of bone differentiation, was evaluated at each time point by mixing an aliquot of culture medium with p-nitrophenyl phosphate (Sigma) at a 1:1 (vol/vol) ratio, and monitoring light absorbance of the mixture at 405 nm over time [13]. ALP activity was calculated from the slope of the absorbance versus time curve.

Cell adhesion/proliferation was characterized at $t=15$ h via fluorescence microscopy and laser scanning cytometry (LSC) [14]. Unbound cells were earlier washed with PBS. The cells were fixed with a 2.5% glutaraldehyde solution in PBS, and the nuclei stained with PIRNase (BD Biosciences). Cell adhesion, spreading and morphology were studied via SEM after fixing and dehydrating the cells in graded ethanol solutions (70%, 80%, 90%, and 100%) and hexamethyldisilazane. A One-way ANOVA and a t-test were used to identify significant differences in cell adhesion/proliferation and ALP activity ($\alpha=0.05$).

3. Results and discussion

3.1. Surface analysis pre-cell seeding

Fig. 1 shows SEM images of the surface morphologies of the coated (A) and oxidized Ti64 (B-D) samples prior to the introduction of HOS cells. Fig. 1A shows the surface image of the TiO_2 coating prior to the heat treatment. The characteristic microstructure of thermal spray coatings is clearly evident. Due to the high velocity of partially molten TiO_2 powders, the surface morphology of the as deposited coatings is rough and contains a distribution of TiO_2 particle sizes. No NWs were present as a result of the thermal spray coating.

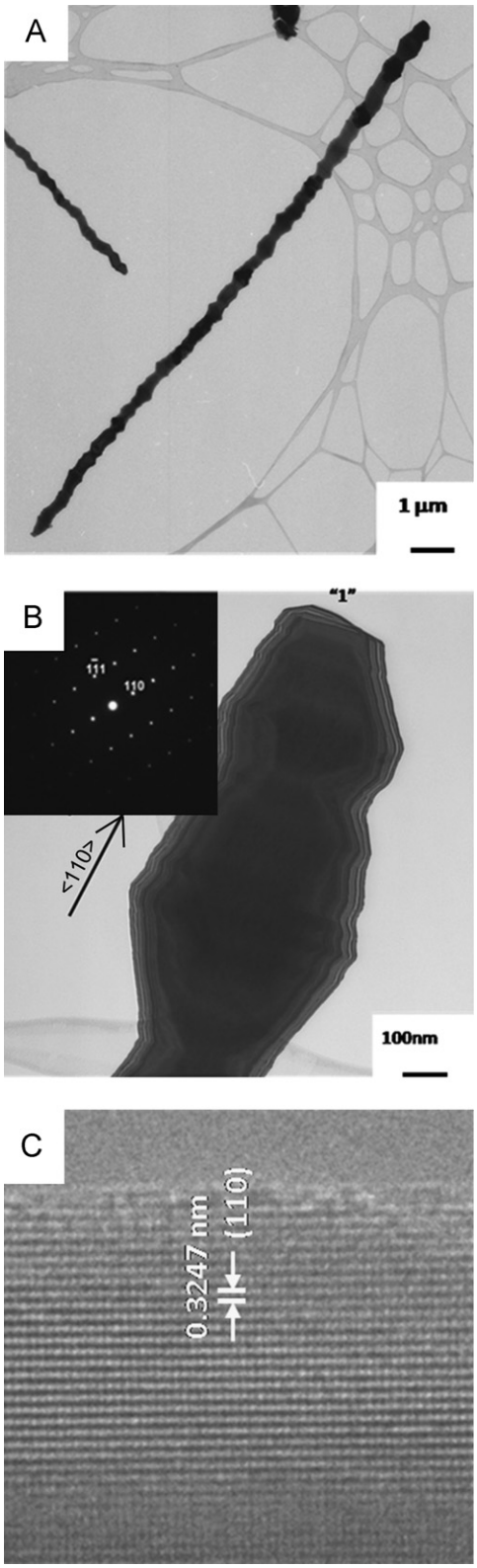

Fig. 2. (A) A BF TEM image showing an individual NW segment, (B) an image showing the tip of the NW and the inset shows the corresponding SAD pattern of the NW and (C) a HRTEM lattice image of the NW.

Fig. 1B shows the surface morphology of the TiO_2 coated Ti64 substrates after a heat treatment in Ar at 700 °C for 8 h. The majority of the nanostructures resulting from the oxidation process were NWs while nanoribbons were also observed. The as grown NWs had the appearance of stacked polyhedrons (Fig. 1C) which were similar to an equilibrium shape of the TiO_2 rutile structure. The NWs formed had irregular distributions in lengths over the range of 2–6 μm. The average diameters of the long acicular nanowires were less than 500 nm. Nanoribbons exhibited smooth top and bottom faces with rippled sides as shown in Fig. 1D.

The phase of nanowires could be determined by XRD; however, because of the thickness of TiO_2 coating (100 μm), the XRD analysis also collects the phase information of the TiO_2 bulk and found it is not suitable for the phase characterization of individual NWs. Therefore, the phase of NWs was analyzed by selected area diffraction (SAD) in an HRTEM. Fig. 2A shows a bright field (BF) TEM image of an individual NW segment. The length and

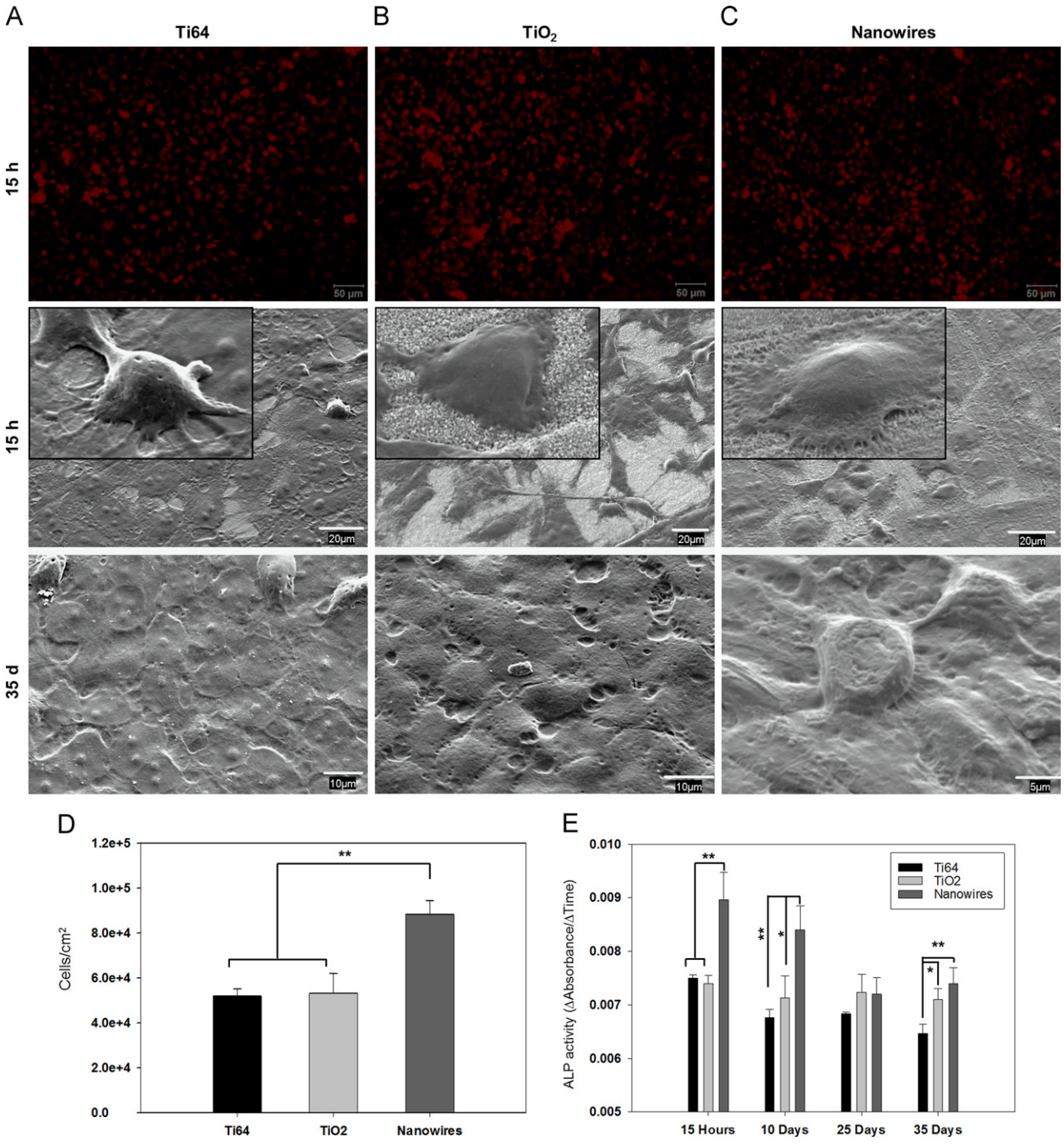

Fig. 3. (A)–(C) Fluorescence (top row), and electron (middle and bottom rows) micrographs of HOS cells cultured on the different surfaces. (D) Cell adhesion/proliferation results. (E) ALP activity results. * and ** indicate $p \leq 0.1$ and $p \leq 0.05$, respectively.

diameter of the nanowire were approximately 6 μm and 300 nm, respectively. A high magnification BF image of the tip is shown in Fig. 2B with its corresponding SAD pattern. No metallic cap was present at the tip of the NW, thus eliminating the popular vapor–liquid–solid (VLS) mechanism as the means of confinement of growth to one dimension [15]. The inset SAD pattern of the tip was indexed to the rutile phase of TiO_2 with a zone axis of $[-112]$. The growth direction of $\langle 110 \rangle$ was obtained from the lattice image presented in Fig. 2C.

3.2. Osteoblast-like cell responses to TiO_2 nanowires

All three Ti64 based substrates were seeded with HOS cells and were subsequently analyzed by SEM and fluorescence microscopy. These observations showed that the cells were able to adhere, spread and proliferate on all three substrates (Ti64, TiO_2, and TiO_2 NWs). Fig. 3 shows fluorescence microscopy images of the nuclei of HOS cells after 15 h of culture. The cells formed a relatively dense monolayer on the surface of each sample. SEM micrographs (Fig. 3A–C) at 15 h did not reveal significant differences in cell morphology between control (Ti64 and TiO_2) and TiO_2 NW surfaces. The cells presented a star-like shape, exhibiting in some cases large cytoplasmic projections, and in some others a uniform radial spreading. HOS cells on TiO_2 nanowires showed abundant filopodia interacting with the surface (Fig. 3C). After 10 days of culture the cells covered the entire surface of all the substrates. Long-term cultures ($t > 10$ days) presented signs of extracellular matrix deposition, and the cells started to exhibit a polygonal-like morphology (Fig. 3A–C), typical of more mature osteoblasts [16]. Although this morphology was found on all the substrates, it tended to be more abundant and defined on the NWs.

LSC characterization (Fig. 3D) revealed improved osteoblast-like cell adhesion/proliferation on TiO_2 NWs, compared to flat Ti64 and TiO_2 substrates ($p=0.012$). Recent reports indicate that nanotextured Ti-based surfaces upregulate the expression of specific bone proteins such as Osteopontin (OPN), Osteocalcin (OCN) and Bone Sialoprotein (BSP) [17–19]. De Oliveira and Nanci (2004) reported early expression of BSP and OPN by osteoblasts cultured on nanostructured Ti surfaces [19]. BSP and OPN are known to contain adhesion-promoting peptide sequences (e.g. RGD), which are believed to trigger important cellular processes, including adhesion, proliferation, differentiation and migration [20–22].

Osteoblast-like cells exhibited increased ALP activity (Fig. 3E) after 15 h and 10 days of culture ($p=0.019$ and 0.042, respectively) on TiO_2 NWs, with respect to flat Ti64 and TiO_2 substrates. ALP activity has been widely recognized as a marker for bone cell functionality [13,23,24]. Expression levels are usually elevated during dynamic extracellular matrix deposition [25]. ALP activity on flat Ti64 and TiO_2 remained relatively constant at any given time point, and was comparable to the baseline value measured on tissue culture polystyrene controls ($\Delta Absorbance/\Delta Time = 0.0077 \pm 0.0002$).

4. Conclusions

Thermal oxidation of TiO_2 coated Ti64 has been shown to produce highly anisotropic 1-D nanostructures. The resulting NWs were found to be the rutile phase of TiO_2 with an $\langle 110 \rangle$ growth direction. The high surface area nanostructured coating was tested for its impact on cell adhesion and proliferation and compared to that of both bare Ti64 and a thermally applied spray coating of TiO_2. TiO_2 NW coated Ti64 samples showed increased cell adhesion and proliferation compared to the spray coated TiO_2 and bare Ti64 substrates. The increased cell growth could be attributed in part to the NWs enhancing cell–substrate interactions.

Acknowledgments

The authors acknowledge Dr. H. Cai of Georgia Institute of Technology for his help with the HRTEM work.

References

[1] J.M. Wu, H.C. Shih, W.T. Wu, Y.K. Tseng, I.C. Chen, Thermal evaporation growth and the luminescence property of TiO_2 nanowires, Journal of Crystal Growth 281 (2005) 384–390.
[2] H.W. Peng, J.B. Li, Quantum confinement and electronic properties of rutile TiO_2 nanowires, Journal of Physical Chemistry C 112 (2008) 20241–20245.
[3] L. Francioso, A.M. Taurino, A. Forleo, P. Siciliano, TiO_2 nanowires array fabrication and gas sensing properties, Sensors and Actuators B—Chemical 130 (2008) 70–76.
[4] G.K. Mor, O.K. Varghese, M. Paulose, K. Shankar, C.A. Grimes, A review on highly ordered, vertically oriented TiO_2 nanotube arrays: fabrication, material properties, and solar energy applications, Solar Energy Materials and Solar Cells 90 (2006) 2011–2075.
[5] H. Tada, F. Suzuki, S. Yoneda, S. Ito, H. Kobayashi, The effect of nanometre-sized Au particle loading on TiO_2 photocatalysed reduction of bis(2-dipyridyl)disulfide to 2-mercaptopyridine by H_2O, Physical Chemistry Chemical Physics 3 (2001) 1376–1382.
[6] Arafat M.M., Dinan B., Akbar S.A., Haseeb ASMA. Gas sensors based on one dimensional nanostructured metal-oxides: a Review, Sensors 12 (2012) 7207–7258.
[7] H. Lee, S. Dregia, S. Akbar, M. Alhoshan, Growth of 1-D TiO(2) nanowires on Ti and Ti alloys by oxidation, Journal of Nanomaterials (2009) 7.
[8] C.N. Elias, J.H.C. Lima, R. Valiev, M.A. Meyers, Biomedical applications of titanium and its alloys, Journal of the Minerals, Metals and Materials Society 60 (2008) 46–49.
[9] G. Balasundaram, C. Yao, T.J. Webster, TiO_2 nanotubes functionalized with regions of bone morphogenetic protein-2 increases osteoblast adhesion, Journal of Biomedical Materials Research Part A 84A (2008) 447–453.
[10] Tan A.W., Pingguan-Murphy B., Ahmad R., Akbar S.A. Review of titania nanotubes: fabrication and cellular response, Ceramics International 38 (2012) 4421–4435.
[11] T. Sun, M. Wang, Mechanical performance of apatite/TiO(2) composite coatings formed on Ti and NiTi shape memory alloy, Applied Surface Science 255 (2008) 404–408.
[12] M. Gaona, R.S. Lima, B.R. Marple, Nanostructured titania/hydroxyapatite composite coatings deposited by high velocity oxy-fuel

(HVOF) spraying, Materials Science and Engineering A—Structural Materials: Properties, Microstructure and Processing 458 (2007) 141–149.
[13] N.N. Ali, J. Rowe, N.M. Teich, Constitutive expression of non-bone liver kidney alkaline phosphatase in human osteosarcoma cell lines, Journal of Bone and Mineral Research 11 (1996) 512–520.
[14] Z. Darzynkiewicz, E. Bedner, X. Li, W. Gorczyca, M.R. Melamed, Laser-scanning cytometry: a new instrumentation with many applications, Experimental Cell Research 249 (1999) 1–12.
[15] R.S. Wagner, W.C. Ellis, Vapor–liquid–solid mechanism of single crystal growth, Applied Physics Letters 4 (1964) 89–90.
[16] C. Morelli, G. Barbanti-Brodano, A. Ciannilli, K. Campioni, S. Boriani, M. Tognon, Cell morphology, markers, spreading, and proliferation on orthopaedic biomaterials. An innovative cellular model for the in vitro study, Journal of Biomedical Materials Research Part A 83A (2007) 178–183.
[17] M.J. Dalby, D. McCloy, M. Robertson, H. Agheli, D. Sutherland, S. Affrossman, et al., Osteoprogenitor response to semi-ordered and random nanotopographies, Biomaterials 27 (2006) 2980–2987.
[18] G. Zhao, O. Zinger, Z. Schwartz, M. Wieland, D. Landolt, BD. Boyan, Osteoblast-like cells are sensitive to submicron-scale surface structure, Clinical Oral Implants Research 17 (2006) 258–264.
[19] de P.T. Oliveira, A. Nanci, Nanotexturing of titanium-based surfaces upregulates expression of bone sialoprotein and osteopontin by cultured osteogenic cells, Biomaterials 25 (2004) 403–413.
[20] L.W. Fisher, D.A. Torchia, B. Fohr, M.F. Young, N.S. Fedarko, Flexible structures of SIBLING proteins, bone sialoprotein, and osteopontin, Biochemical and Biophysical Research Communications 280 (2001) 460–465.
[21] G.B. Schneider, R. Zaharias, C. Stanford, Osteoblast integrin adhesion and signaling regulate mineralization, Journal of Dental Research 80 (2001) 1540–1544.
[22] T.V. Byzova, W. Kim, R.J. Midura, E.F. Plow, Activation of integrin alpha(v)beta(3) regulates cell adhesion and migration to bone sialoprotein, Experimental Cell Research 254 (2000) 299–308.
[23] S. Ozawa, S. Kasugai, Evaluation of implant materials (hydroxyapatite, glass-ceramics, titanium) in rat bone marrow stromal cell culture, Biomaterials 17 (1996) 23–29.
[24] H.W. Kim, S.Y. Lee, C.J. Bae, Y.J. Noh, H.E. Kim, H.M. Kim, et al., Porous ZrO_2 bone scaffold coated with hydroxyapatite with fluorapatite intermediate layer, Biomaterials 24 (2003) 3277–3284.
[25] K.C. Popat, L. Leoni, C.A. Grimes, T.A. Desai, Influence of engineered titania nanotubular surfaces on bone cells, Biomaterials 28 (2007) 3188–3197.